Cell Research (2011) 21:338-349.

www.nature.com/cr

ORIGINAL ARTICLE

Pulse labeling and long-term tracing of newborn neurons in the adult subgranular zone

Xuewen Cheng[1], Yang Li[1], Ying Huang[1], Xiaoyan Feng[1], Guoping Feng[2], Zhi-Qi Xiong[1]

[1]Institute of Neuroscience, State Key Laboratory of Neuroscience, Shanghai Institutes for Biological Sciences, Chinese Academy of Sciences, 320 Yueyang Road, Shanghai 200031, China; [2]Department of Brain and Cognitive Sciences, McGovern Institute, Massachusetts Institute of Technology, 77 Massachusetts Avenue, Cambridge, MA 02139, USA

Research over the past decades has demonstrated that adult brain produces neural progenitor cells which proliferate and differentiate to newborn neurons that integrate into the existing circuit. However, detailed differentiation processes and underlying mechanisms of newly generated neurons are largely unknown due to the limitation of available methods for labeling and manipulating neural progenitor cells and newborn neurons. In this study, we designed a tightly controlled, noninvasive system based on Cre/*lox*P recombination to achieve long-term tracing and genetic manipulation of adult neurons *in vivo*. In this system, tamoxifen-inducible recombinase, CreER^{T2}, was driven by BAC-based promoter of doublecortin (DCX, a marker of newborn neurons). By crossing this Cre line with reporter mouse, we found that newborn neurons in the dentate gyrus (DG) could be selectively pulse-labeled by tamoxifen-induced expression of yellow fluorescent protein (YFP). YFP-positive neurons were identified by coimmunostaining with cell type-specific markers and characterized by electrophysiological recording. Furthermore, analysis of the migration of these neurons showed that the majority of these labeled neurons migrated to the inner part of granule cell layer. Moreover, spine growth of inner molecular layer of newborn granule neurons takes a dynamic pattern of invert U-shape, in contrast to the wedge-shaped change in the outer molecular layer. Our transgenic tool provides an efficient way to selectively label and manipulate newborn neuron in adult mouse DG.

***Keywords*:** adult neurogenesis; doublecortin; genetic labeling; dentate gyrus; spine

Cell Research (2011) **21**: 338-349. doi:10.1038/cr.2010.141; published online 12 October 2010

Introduction

In the adult brain, neural stem cells remain active in discrete brain niches such as subgranular zone (SGZ) of the dentate gyrus (DG) and subventricular zone (SVZ) of the lateral ventricle [1, 2]. These stem cells give rise to neural progenitor cells, which in turn become either glutamatergic or GABAergic neurons. During the past decades, intensive studies of neurogenesis have greatly expanded our knowledge about the survival, differentiation and integration of adult stem cells and newborn neurons [3-5]. These newborn neurons probably play important roles in odor discrimination, learning and memory, and information processing [6-10]. However, the molecular and cellular mechanisms underlying the development of neuronal progenitor cells and circuit integration of newborn neurons are largely unknown.

Newborn neurons generated in the SGZ migrate into the granule cell layer (GCL) and develop apical dendritic tree and axon branches [11, 12]. The dendritic field of granule neuron can be divided into three sub-layers [13]. Spine structure in the inner molecular layer (IML) has long been considered mainly as postsynaptic partner of mossy cells, and this connection is important for modulation of granule cell excitability and plasticity [13-16]. Recent work found a semilunar granule cells (SGC)-relayed pathway, which recruit mossy cells to refine directly and indirectly the firing of distinct granule cell populations [17]. This finding provides new evidence to support the important role of synaptic connection of the IML in the regulation of granule neuron function. Although spine development of adult newborn neurons in

Correspondence: Zhi-Qi Xiong
Tel: +86-21-54921720; Fax: +86-21-54921735
E-mail: xiongzhiqi@ion.ac.cn
Received 11 April 2010; revised 12 July 2010; accepted 17 August 2010; published online 12 October 2010

the outer molecular layer (OML) has been described [18], spine development in the IML is still unknown.

Recent progress in generating transgenic mouse lines facilitated the labeling and analysis of adult neural stem cells and newborn neurons. However, in traditional transgenic lines [19], reporter genes driven by transient marker gene promoters are only expressed temporally in immature stage, thus making genetic manipulation and long-tem tracing of newborn neurons difficult. Transgenic mice expressing inducible recombinase ($CreER^{T2}$) [20] in neuronal stem or precursor cells provide new approaches to neurogenesis labeling and manipulation [10, 21]. However, these mice cannot be used for pulse labeling of a large population of newborn neurons at a defined time period, due to high $CreER^{T2}$ activity in proliferating stem cells or progenitor cells. This caveat makes them not suitable for stringent study of differentiation kinetics of neurogenesis, especially for long-term tracing and manipulation of newborn neurons generated at certain life time. Retrovirus that lacks nuclear import mechanism can specifically infect dividing mammalian cells [22], and thus enables the labeling at a defined birth date. However, high-titer virus preparation needs experienced skills, and inflammation and variation of viral injection between animals can always be the issues. These limitations of present approaches entail the development of new tools to study adult neurogenesis.

Here, we describe a new transgenic tool in which the activity of $CreER^{T2}$ driven by doublecortin (*dcx*) promoter was induced specifically in postmitotic newborn neurons of the adult DG. Specificity of labeling was validated by coimmunostaining with markers of proliferating progenitors, nondividing newborn neurons and mature neurons, and characterized by electrophysiological recording. The yellow fluorescent protein (YFP)-positive (YFP^+) neurons were studied from 5 days to several months post induction, and the migratory pattern and dendritic outgrowth were analyzed. Most YFP^+ neurons migrated into the inner GCL (iGCL). Moreover, in contrast to the steady increment of spine density in the OML [18], spine density at the IML increased first and decreased 1 month after induction. These findings provide a morphological basis for functional integration of newborn neurons into the working circuit in adult brain.

Results

YFP-labeled cells localize specifically in SGZ and are postmitotic newborn neurons in adult brain

We selected *dcx* promoter to drive the expression of $CreER^{T2}$ in early newborn neurons, as DCX is well characterized to be restricted in immature newborn neurons of adult brain [23-25], and its expression is relatively stable under various stimulation conditions compared with other known transient markers such as PSA-NCAM and CRAMP4 [3, 26]. We used a bacterial artificial chromosome (BAC) clone [27] that contains the entire *dcx* promoter and gene sequence to build $CreER^{T2}$-expressing construct for transgenic founder production. Founders were initially crossed to *Rosa26-LacZ* reporter mice. Founders that bear *LacZ* expression in neurogenic regions, both in embryonic stage (Supplementary information, Figure S1) and adult DG, were used for further identification.

As YFP is good for immunofluorescence analysis and morphology study [28], *Dcx-CreER^{T2}* mice were then crossed to *Rosa-loxp-STOP-loxp-EYFP* mice (*Rosa26-EYFP* reporter) [29] (Figure 1A). Mice (8 or 9 weeks old) were given tamoxifen, and YFP expression pattern was examined 5 days or 14 days post induction (dpi). Offspring of founder DC-F18 were used for the following experiments. We found that YFP-expressing cells in tamoxifen-induced mice were restricted in the SGZ of the DG (Figure 1C), whereas control mice injected with oil (vehicle) did not show any YFP^+ cells (Figure 1D), indicating that $CreER^{T2}$ activity is specifically induced in the SGZ of hippocampal formation (Figure 1E and 1F). However, no YFP^+ cells were found after repeated tamoxifen induction in the SVZ (Supplementary information, Figures S2 and S3), a region known to generate newborn neurons that mature to become granule cells in the olfactory bulb [30]. In addition, nonspecific YFP-expressing neurons were found within piriform cortex, amygdala and hypothalamus (Supplementary information, Figure S4), areas generally believed to be non-neurogenic [31-33].

We next conducted a series of experiments to characterize the YFP^+ cells in the DG. To examine whether these YFP^+ cells were newly born, 2 months old *Dcx-CreER^{T2}:Rosa26-EYFP* mice were treated with BrdU for 2 days. After 3 days, the mice were induced with tamoxifen for 5 days (Figure 1B). At 14 dpi, we found that YFP-expressing cells in the SGZ colocalized with BrdU, indicating that these cells were newly generated (Figure 2A and 2C). However, they did not express Ki67, a proliferating cell marker, or Tbr2, a specific marker of transient-amplifying precursor cells, suggesting that YFP^+ cells were no longer proliferating precursors (Figure 2A). We also found that most of these YFP^+ cells expressed DCX (Figure 2B), a marker protein expressed in immature neurons. Increasing the duration of tamoxifen induction to 10 days led to additional labeling of more newborn neurons in the DG (Supplementary information, Figure S5). Moreover, YFP^+ cells in the DG exhibited

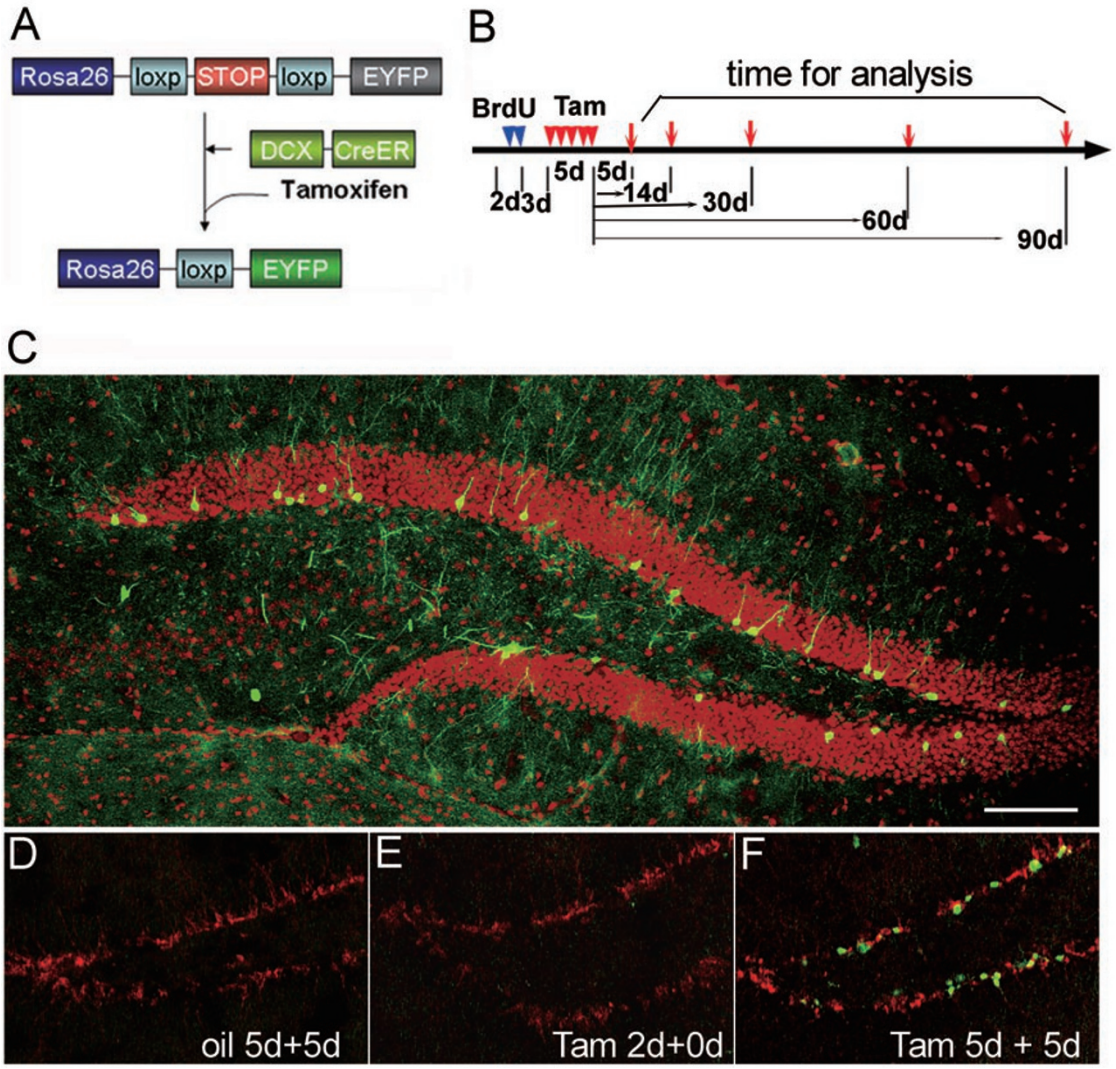

Figure 1 Expression of CreER^{T2} activity in the SGZ of the adult hippocampal DG. **(A)** Schematic depiction of the strategy used to label CreER^{T2} activity-expressing cells with an EYFP reporter. **(B)** Diagram showing the time course of BrdU and tamoxifen induction and schedule of analysis of adult *Dcx-CreER^{T2}:Rosa26-EYFP* mice. Each arrowhead represents 2 injections in 1 day. The red arrows at the right hand indicate the time when a group of induced mice were killed for analysis. **(C)** Low magnification view showing distribution of YFP$^+$ cells (green) in the SGZ. The image was taken from a *Dcx-CreER^{T2}:Rosa26-EYFP* mouse sacrificed 14 days after 5 days of tamoxifen injection. Cell nuclei were counter-stained with Hoechst (red). Scale bar: 100 μm. **(D-F)** CreER^{T2} activity in the SGZ of mice given oil **(D)**, 2 days of tamoxifen **(E)**, or 5 days after 5 days of tamoxifen induction **(F)**. Samples were coimmunostained for YFP (green) and DCX (red).

morphologies typical of newborn neurons, with a rudimental apical dendrite, small round soma and few basal dendrites (Figure 2C). These results demonstrated that YFP$^+$ cells were postmitotic newborn neurons.

Almost all the newborn neurons generated in the adult SGZ were believed to differentiate into glutamatergic granule neurons [34]. To further validate this and to find out whether YFP$^+$ cells also expressed specific markers of differentiated neuronal subtypes, we performed immunostaining against marker proteins of mature neurons (NeuN), astrocytes (GFAP) and interneurons (GAD65/67, parvalbumin). We found that 53.8% YFP$^+$ cells in the SGZ were mature neurons (NeuN$^+$, Figure 2A and 2B), and none were astrocytes (GFAP$^+$). Only an extremely small number of YFP$^+$ cells were GABAergic neurons (GAD65/67, Figure 3A, shown by red arrow). We found that antibodies to GAD65 or GAD67 do not work well in mouse brain slices. To further confirm our observation, we injected BrdU into *GAD67-GFP* (knockin) mouse, and analyzed possible co-labeling at 7 (Figure 3B, top

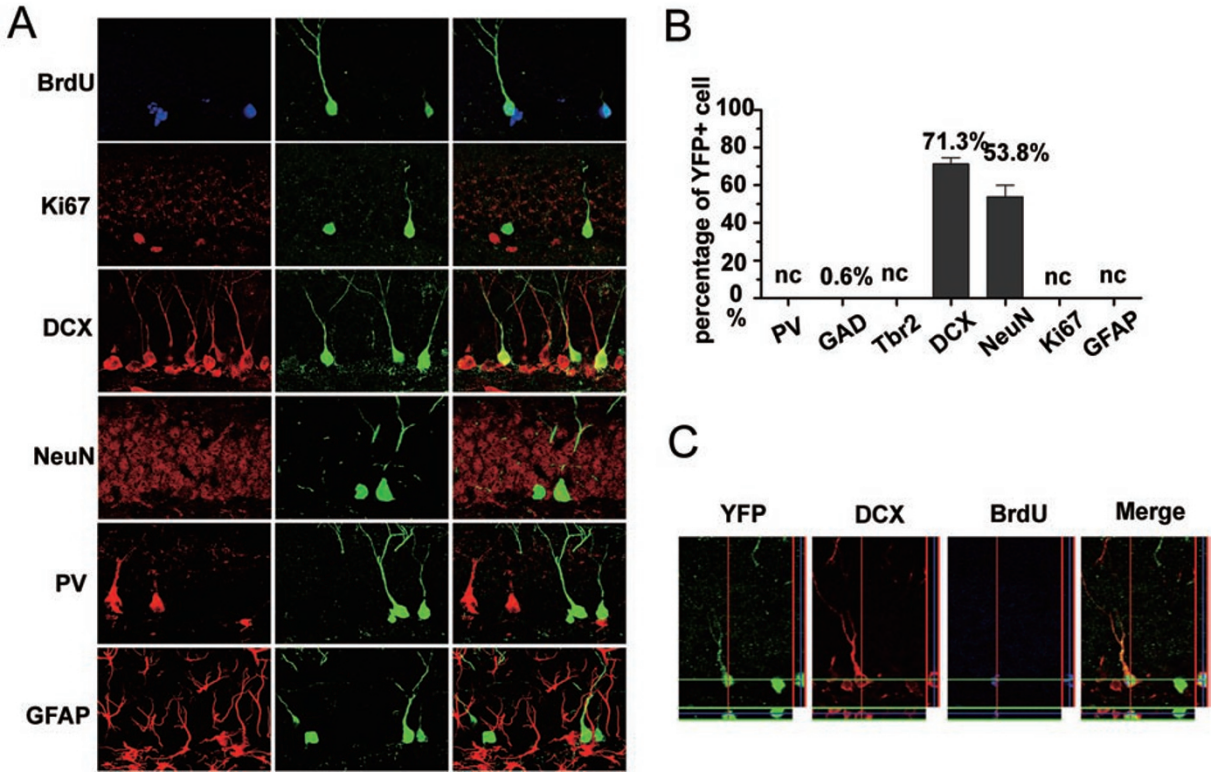

Figure 2 Specific labeling of postmitotic newborn neurons by *Dcx-CreER*^{T2} in the adult DG. **(A**, **B)** Identification of YFP$^+$ cell types. BrdU was administered to mice 3 days before tamoxifen treatments. At 14 dpi, slice samples were immunostained for the cell type maker indicated (red). YFP was visualized by anti-GFP immunostaining in all cases, except in sections labeled with anti-Ki67 and anti-Tbr2 antibodies. The analysis was done from mice 14 days after 5 days of tamoxifen induction. BrdU was given 3 days before tamoxifen delivery. Abbreviation: DCX, doublecortin; PV, parvalbumin; GFAP, glial fibrillary acidic protein; and Tbr2, T-box brain 2, also known as Eomesodermin. **(B)** Percentage of YFP$^+$ cells in the DG coexpressing the indicated marker protein. "nc" means no colocalization. **(C)** Orthogonal section showing a newborn neuron labeled with YFP (green), DCX (red) and BrdU (blue).

row) or 40 dpi (Figure 3B, bottom row). Similar to our above discovery, only a few BrdU$^+$ cells expressed GFP (3 cells in total 10 slices) (Figure 3B, shown by red arrow and magnified at the right), indicating that very few neurons born in the adult DG are GABAergic. Together, these results revealed that YFP$^+$ cells were pulse-labeled postmitotic newborn neurons, most of which were not GABAergic.

Electrophysiology characterization of YFP-labeled cells

Compared with mature neurons, immature neurons in the GCL have distinct features in excitability and membrane constants due to differential expression of ion channels and transmitter receptors [35, 36]. To analyze the electrophysiological properties of YFP$^+$ cells in the DG, we performed whole-cell patch clamp study at 14 and 28 dpi, and on mature neurons (unlabeled granule cell). We measured the input resistance (R_{in}), firing of action potential, as well as passive membrane property as previously described [35] (Figure 4A). We found at 14 dpi, YFP$^+$ cells in the SGZ had a significantly higher R_{in} (1.32 ± 0.15 GΩ) than YFP$^+$ cells at 28 dpi (535.6 ± 21.1 MΩ) and mature granule neurons (505.2 ± 21.4 MΩ, Figure 4B). Previous studies reported that granule cells in adult rat have an R_{in} within 200-300 MΩ [35]. It seems that the R_{in} value of mouse granule cells is higher than that of rat granule cells [37]. We confirmed the R_{in} value of granule cells in adult rat. Moreover, we tested the R_{in} value of granule cells in adult mice by two independent laboratories, which is indeed higher than that in adult rat (Supplementary information, Figure S6 and Table S1). Newborn neurons expressing PSA-NCAM had been reported to have an R_{in} over 1.5 GΩ [35]. As DCX and PSA-NCAM have very similar expression dynamics in newborn neurons of the DG [38], our result indicated that at 14 dpi, some YFP$^+$ neurons were at a late stage

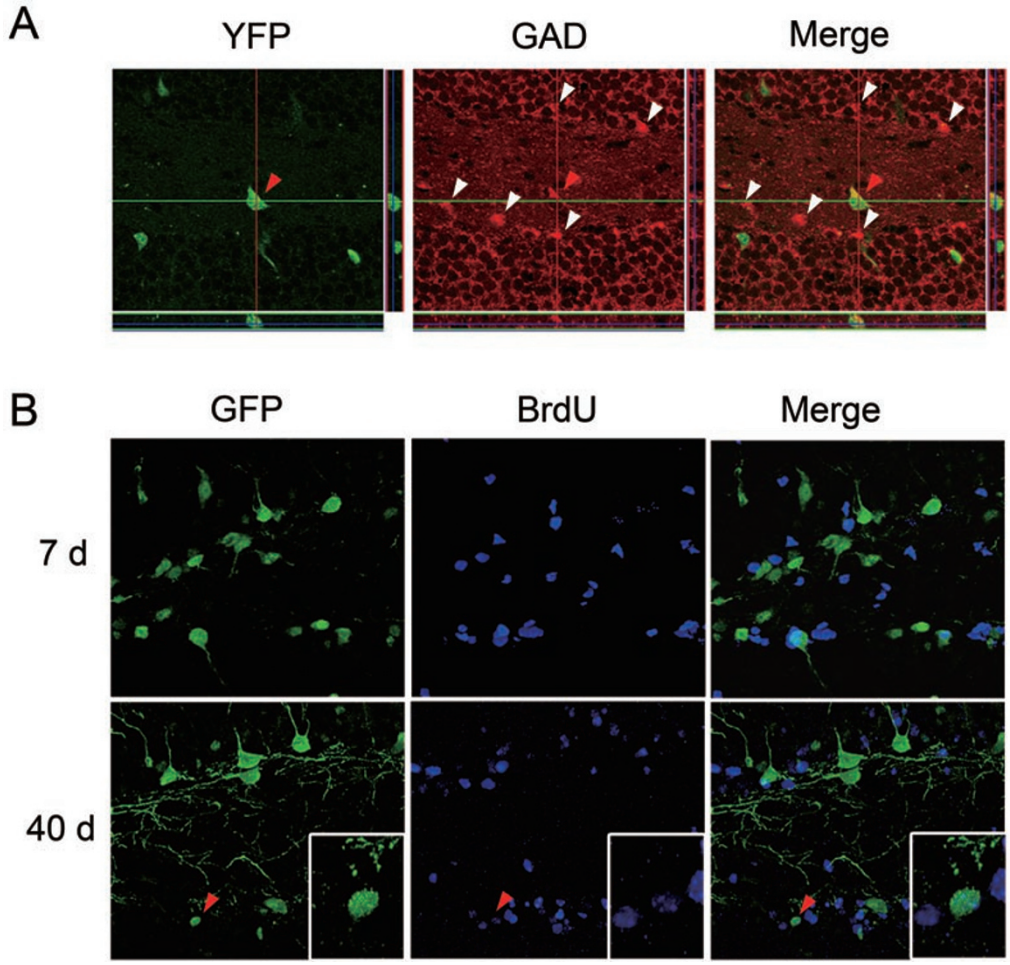

Figure 3 Coimmunostaining of YFP$^+$ newborn neurons with GABAergic neuron markers. **(A)** Coimmunostaining of slices for YFP (green) and GAD65/67 (red). The white arrowheads indicate GAD65/67-positive cells that do not express YFP and the red arrowhead points to an YFP$^+$ cell which colocalizes with GAD65/67. This analysis was done using mice 30 days after tamoxifen induction. **(B)** Colocalization of BrdU (blue) and GFP (green) in *GAD67-EGFP* knockin mice. Top row: immunostaining of GFP and BrdU in slices of *GAD67-EGFP* mice 7 days after BrdU injection. Bottom row: immunostaining of GFP and BrdU in slices of *GAD67-EGFP* mice 40 days after BrdU injection. The inset shows a high magnification view of the area indicated by the red arrow.

of differentiation, consistent with the above observation that 71.3% of YFP+ cells expressed DCX at 14 dpi (Figure 2B). Furthermore, R_{in} values were highly variable in the 2 weeks group, which was probably due to the fact that DCX is expressed in 1- to 3-week-old new neurons, but they become very similar in the 4 weeks group (Figure 4B and 4C), suggesting that our labeling of newborn neurons is pulse labeling.

In addition, we found that action potential was easily induced in YFP$^+$ cells, with a lower threshold current, 28.7 ± 2.9 pA, in labeled neurons at 14 dpi, compared with 64.3 ± 2.0 pA in labeled neurons at 28 dpi and 70.0 ± 4.5 pA in mature granule cells (Figure 4C). Atypical AP firing pattern could be observed in newborn neurons (Figure 4A). Furthermore, young neurons had a higher voltage change evoked by step current injection (Figure 4D) and a slower membrane time constant (14 dpi: 82.7 ± 7.3 ms, 28 dpi: 52.4 ± 8.2 ms, mature: 34.9 ± 1.5 ms) (Figure 4E). These electrophysiological findings are consistent with previous characterization of newborn neurons [35], and thus further consolidated our immunohistochemical findings that YFP$^+$ cells are real newborn neurons.

YFP-labeled cells undergo continuous differentiation into mature neurons

Most newborn neurons generated in the SGZ take 2-4 weeks to migrate radially into the GCL [12]. To test

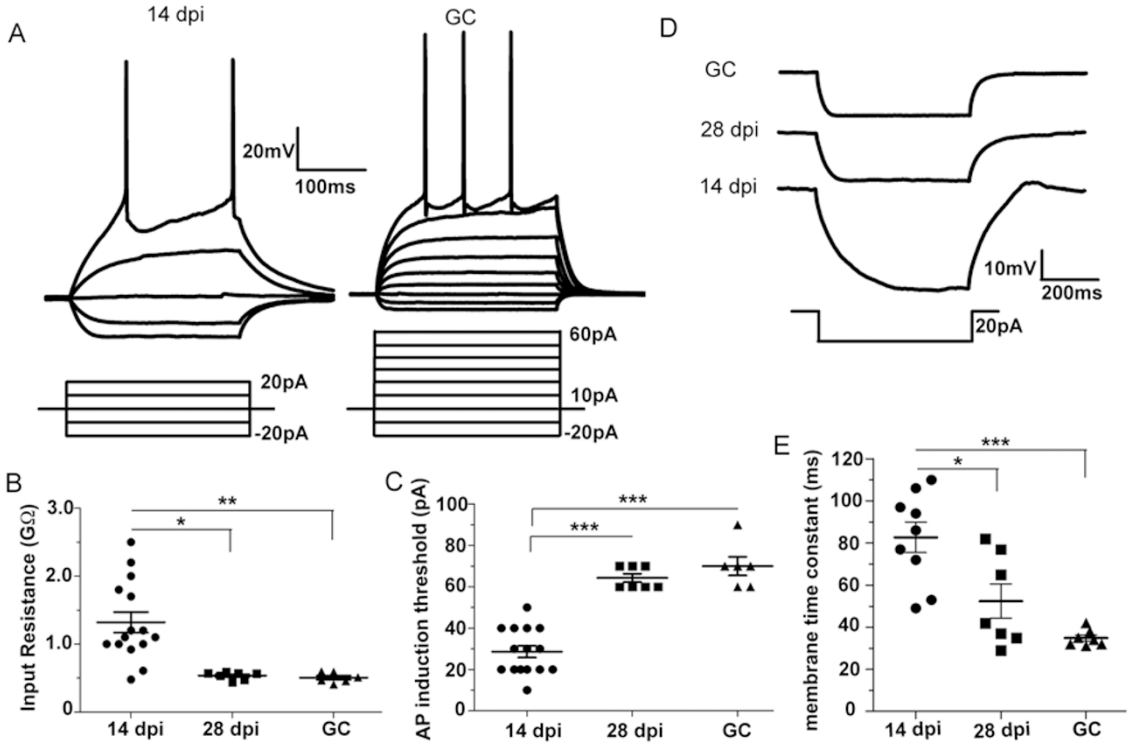

Figure 4 Electrophysiological recordings of YFP$^+$ neurons at 14 and 28 days after tamoxifen induction. **(A)** Representative traces of action potential (AP) spikes elicited from 14 dpi YFP$^+$ neurons and mature granule neurons in the DG. **(B)** Individual and mean input resistance values for 14 and 28 dpi YFP$^+$ neurons and mature granule neurons. **(C)** Individual and mean AP threshold value of YFP$^+$ neurons and mature granule neurons. **(D)** Sample traces of current-evoked changes in membrane potential in 14 and 28 dpi neurons and mature granule neurons. **(E)** Statistical distribution of membrane time constants for 14 and 28 dpi YFP$^+$ neurons and mature granule neurons. ***P < 0.001, **P < 0.01, *P < 0.05. Abbreviations: dpi, days post induction.

whether and how these YFP$^+$ cells continued their development, we used stage-specific markers to classify their immature or mature identity at 5, 14, 30, 60 and 90 dpi (Figure 1B). At 5 dpi, the soma of most YFP$^+$ cells was localized within the SGZ (Figure 5A and 5C), and 85.1% of YFP$^+$ cells were DCX$^+$ and 27.8% colocalized with mature neuron marker NeuN (Figure 5B). At 14 dpi, some YFP$^+$ cells migrated into the iGCL (Figure 5C). A total of 70.7% of YFP$^+$ cells still coexpressed DCX and 54.7% expressed NeuN. By 30 dpi, all the YFP$^+$ cells became NeuN$^+$ and DCX$^-$ (Figure 5A and 5B), indicating that they were fully differentiated. At 60 dpi, the soma of YFP$^+$ cells continued to migrate into the GCL, with some of them ending up in the outer GCL (oGCL) (Figure 5C). At 90 dpi, most of the somas were localized in the iGCL, with a small proportion of cell soma reaching the oGCL (Figure 5C).

Since DCX is transiently expressed within several days up to 3 weeks once a neuron is born [23], the population of YFP$^+$ cells at a certain time point may include neurons with an age that varies from days to weeks. This difference may underlie the observed diversity of neuronal morphology and maturation status. By combining CreER^{T2}-mediated recombination with BrdU incorporation, which enables labeling a population of newborn neurons with defined birth date, we were able to narrow down the birth dates in a strict time window to achieve the homogeneity of neurons for morphological analysis and genetic dissection. Mice (2-3 months old) were administered with BrdU for 2 days. After 3 days, these mice were further injected with tamoxifen for 5 days and sacrificed 10 days later. Approximately 75% of all YFP$^+$ cells expressed DCX, whereas all YFP$^+$/BrdU$^+$ cells also expressed DCX, indicating that these cells born 19-20 days ago are all DCX positive (DCX$^+$). Moreover, among all the YFP$^+$ cells, as many as 21.4% of them are BrdU$^+$, indicating these YFP$^+$ cells were born during the BrdU incorporation period.

In terms of the number of YFP-labeled cells at each time point [12, 39, 40], we observed a slight increase

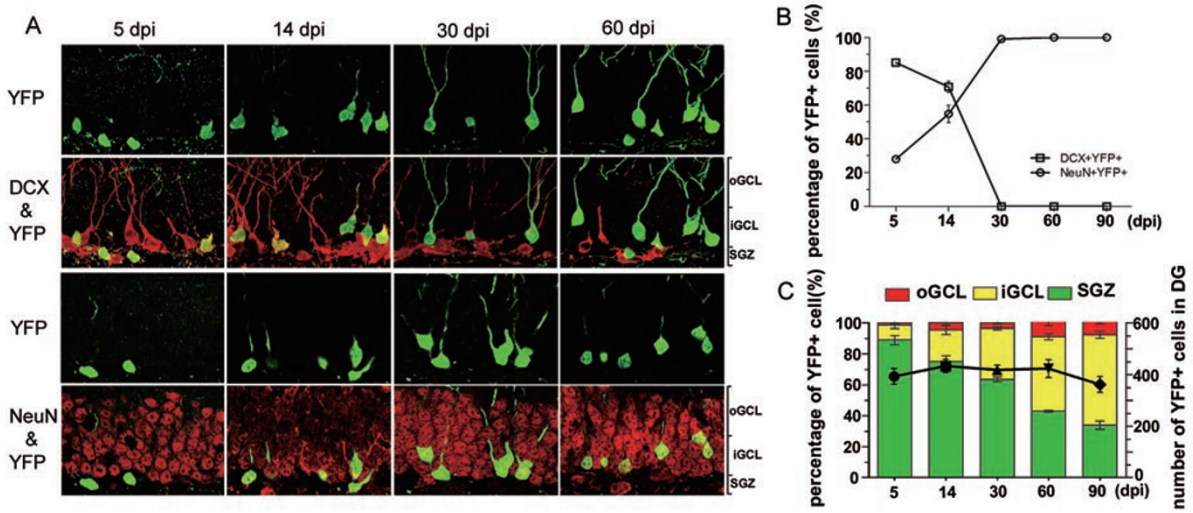

Figure 5 YFP$^+$ neurons underwent continuous differentiation and migrated into the GCL. Tamoxifen induction paradigm was shown in Figure 1B. **(A)** Coimmunostaining of YFP with newborn neuron marker (DCX) or mature neuron marker (NeuN) at the indicated time points. Images of DCX and YFP are reconstructed from z-series by three-dimension projection. Images of NeuN and YFP were single plane of Z series stack. The GCL was divided into outer GCL (oGCL), inner GCL (iGCL) and subgranular zone (SGZ), as indicated on the right hand side. **(B)** Proportions of DCX$^+$ neurons (immature) and NeuN$^+$ neurons (mature) among YFP$^+$ neurons at indicated time points. **(C)** Left *y*-axis: distribution of YFP$^+$ cell soma in the GCL at the time points indicated. Right *y*-axis: average number of YFP$^+$ cells in the DG at each time point. Abbreviation: dpi, days post induction.

(~10%) from 5 to 14 dpi (Figure 5C, dot line, right axis). This was probably due to the lag time between Cre-mediated recombination and the accumulation of YFP protein within the cell. From 14 to 90 dpi, the average number of YFP$^+$ cells decreased only slightly, indicating that the majority of YFP$^+$ newborn neurons survived this period (Figure 5C). The decrease could be due to either slight variability between tamoxifen injections or apoptosis of neurons that failed to integrate into the working circuit. As YFP signal at early time is not strong enough, our tool is not suitable for survival analysis shortly after tamoxifen induction.

YFP-labeled neurons extend dendrite into the IML and form spines

Newborn neurons from the adult SGZ not only migrate but also undergo morphological changes. The current understanding of these morphology changes comes mostly from studies using transiently expressed marker protein or virus infection. Our genetic tool enables us to permanently label newborn neurons of mice at any given time point. As EYFP expression in *Rosa26-EYFP* reporter mice was not robust, *Dcx-CreER^{T2}* mice were crossed to *thy*1-*EYFP* reporter to examine dendrite and spine morphogenesis [41]. At 2 weeks after injection, *thy*1 promoter-driven expression of EYFP was strong enough to enable long-term tracing and analysis of dendritic spines (Figure 6B).

The dendritic field of granule neuron, known as the molecular layer (ML), can be divided into three sublayers [42]. The widest layer, middle molecular layer (MML), receives projections from layer III pyramidal neurons of the entorhinal cortex, while the IML, which is situated between the MML and the GCL, receives mainly excitatory input from mossy cells [15]. During our screening of founder lines, we found that a Cre line, named DC-F30, had ectopic recombination activity in cortical plate. In contrast to DC-F18, which did not express CreER^{T2} activity in the cortex, DC-F30 offspring showed robust expression of tamoxifen-induced recombination activity in layer III, IV and VI of the cortex (Figure 6A, left), and some of the neurons from these layers projected to the DG through the perforant pathway (Figure 6A, right). The evident expression of YFP in cortical axons within the OML simplified the delineation of dendritic fields in the molecular layer, thus facilitating the analysis of spine differentiation in the IML (Figure 6A, right).

New granule neurons born in the adult SGZ generate dendritic spines at the age of 16 days, with a 4-day delay compared with that of neurons born during embryonic development [18]. We observed that spine density in

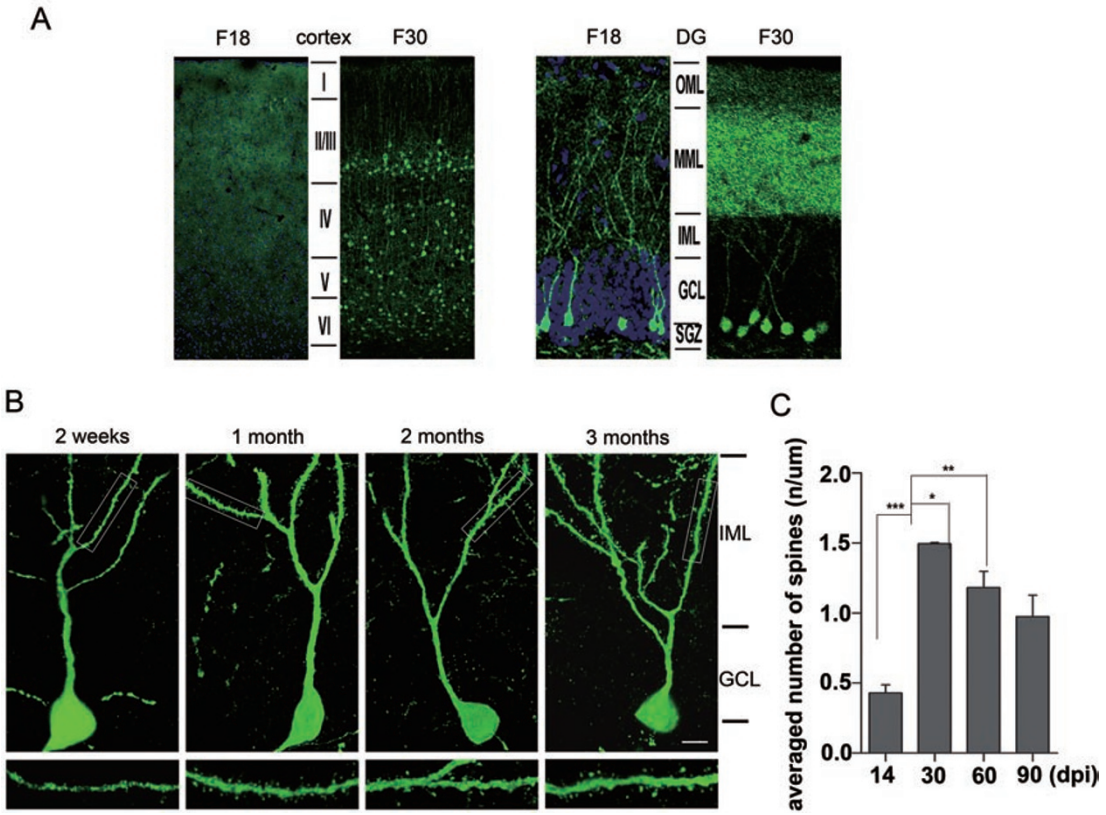

Figure 6 Spine density analysis of YFP$^+$ neurons in the inner molecular layer (IML) of adult DG. **(A)** Comparison of YFP expression in the cortex and DG of DC-F18 and DC-F30 lines. Sections were counter-stained with Hoechst. Cortical (left hand panels) and DG (right hand panels) layer boundaries are indicated. **(B)** Dendritic architecture of YFP$^+$ neurons in the IML at indicated time points. Higher magnification views of the segments within the white rectangles are shown at bottom. Scale bar: 5 μm. **(C)** Statistical analysis of spine density on IML dendrites of YFP$^+$ neurons at different time points. ***P < 0.001, **P < 0.01, *P < 0.05. Abbreviation: OML, outer molecular layer; MML, middle molecular layer; IML, inner molecular layer; GCL, granule cell layer; SGZ, subgranular zone; dpi, days post induction.

YFP$^+$ granule neuron dendrite of the MML and OML was similar to that reported previously (data not shown) [18]. However, this was not the case for the IML, where the density of spines increased from 4.30 spines per 10 μm at 14 dpi to 14.95 spines per 10 μm at 30 dpi (Figure 6B and 6C). Subsequently, spine density decreased to 11.82 spines per 10 μm at 60 dpi and 9.75 spines per 10 μm at 90 dpi, suggesting that these neurons undergo a process of synaptic pruning.

Discussion

In this study, we report a new inducible genetic tool for specific labeling of newborn neurons or ablation of interested gene in the adult hippocampal DG. The CreER^{T2} recombinase driven by *dcx* promoter is expressed in postmitotic newborn neurons. This tool allows reliable pulse labeling of early neurons born within a short time window during adulthood, thereby facilitating the analysis of differentiation and integration of adult-born new neurons at specific time points. Using this tool, we have also tracked the migration of these labeled newborn neurons from the SGZ to the GCL over months, during which time they sequentially expressed stage-specific marker proteins and developed morphology of destined neuron subtypes. Specifically, the dendritic spines at the MML and IML take different differentiation patterns. In contrast to the gradual increase of spines in MML (wedge shaped), spines in IML increase during the first month after induction and then decrease.

Compared with *Nestin-CreER^{T2}* mouse [21], in which YFP-labeled cells can generate daughter precursor cells over months, our *Dcx-CreER^{T2}* system provides more precise information about the age of labeled neurons. Unlike retrovirus labeling techniques, our tool can readily be used for both labeling and genetic manipulation, thus

providing a noninvasive approach to neurogenesis study for those labs that are not experienced in virus packaging. Moreover, the efficiency and specificity is more reliable than virus infection. Genetic labeling using our system excludes nonspecific labeling of other dividing cells using virus infection [43], hence our tool is better for more stringent study of neurogenesis. However, due to the nonspecific recombination activity in other brain regions outside DG, our tool may not be appropriate for studies of neurogenesis with behavioral outcomes.

Neuronal progenitors generated in the DG can be categorized into three types, with type 2b and type 3 cells expressing DCX [44]. Although type 2b and type 3 cells are capable of proliferating, it does not mean that CreER^{T2} is expressed in these cells. According to our observation that no YFP$^+$ cells expressed Ki67, Tbr2 and sox2, it may be interpreted that CreER^{T2} activity is above the threshold for recombination only in postmitotic immature neurons. This feature allows dissection of neurogenesis process into two stages—proliferation and differentiation. For functional study of genes that participate in both stages, our genetic tool can specifically knock out the gene in differentiation stage to achieve more stringent analysis.

The observation that 85% of YFP-labeled cells are DCX$^+$ at 5 dpi reveals that our labeling system targets newborn neurons during a time window of several days to 3 weeks. Previous study of PSA-NCAM$^+$ neurons in the DG found that these neurons have a mean R_{in} value over 3.0 GΩ. In our electrophysiological experiments, YFP$^+$ cells at 14 dpi had a mean R_{in} value of 1.3 GΩ, and 71.3% of them were DCX$^+$. Together with previous observation that DCX is expressed in immature neurons as old as 3 weeks, these findings led us to speculate that CreER^{T2} is activated by tamoxifen mostly (70%) in new neurons generated within 10 days. In combination with BrdU labeling, our transgenic tool can achieve permanent labeling and genetic manipulation of adult newborn neurons with defined birth date.

Based on our observation and previous reported data, most neurons born in the SGZ are added into the iGCL [10, 12]. Thus, granule neurons in the oGCL may undergo turnover with a much slower rate compared with those in iGCL, which may lead to differential plasticity properties between these two parts. Furthermore, neurons in the iGCL may have distinct fiber innervation compared with neurons in the oGCL.

We observed that dendritic architecture of the newborn neurons became much complex during the several months after birth. Dendritic spines function as the postsynaptic structures for excitatory synapse [45]. The complete integration of newborn neurons into circuits involves not only forming connection with axons of cortical neuron, but also with mossy cells in the hippocampus and interneurons in hilar region [46]. Synapse formed with mossy cell stands for another excitatory input into new granule neurons [15]. Mossy cell input mediated critical regulation of granule excitability by activities from distant granule cells of ipsilateral hippocampus [13, 16]. This connection was also important for the maintenance of NMDA-dependent long-term potentiation [14]. Based on our transgenic technique to dissect MML and IML, we specifically analyzed spine differentiation of IML. We found that the total spine density of IML increased first and decreased later, which was similar to the spine density change of newborn neurons generated in neonatal brain. It is known that the decrease of spine density can be indicative of competition between spines to synapse with a presynaptic partner, and only those receiving presynaptic input can survive and mature [46]. Thus, the dynamics of spine density changes on dendrites in the IML may be driven by activity-dependent regulation of mossy cell-granule cell synapse development and highlights the complicated process of circuit integration of newborn granule neurons.

Materials and Methods

Generation of BAC transgenic mice

To generate transgenic mice expressing CreER^{T2} under the control of the *dcx* promoter, we selected a BAC clone (RP23-462G16, Rosewell Park Cancer Institute) encompassing the *dcx* gene (90 kb), as well as 30 kb upstream and 60 kb downstream of the locus. To make targeting sequence, two homologous arms of the *dcx* gene were inserted into the CreER^{T2} plasmid pERFN, which consists of the CreER^{T2} open reading frame (ORF), a BGH poly(A) tag and an *FRT* element-flanked *Neo*-resistant cassette in a pBluescript vector. Homologous recombination between *dcx* BAC clone and the CreER^{T2} targeting fragment was then carried out using a defective prophage system. The use and storage of plasmid was guided by NIH guidelines for research involving recombinant DNA molecules. For more information, please see Supplementary information, Data S1.

Tamoxifen and BrdU administration

Tamoxifen is diluted in corn oil at 20 mg/ml. For embryonic administration, pregnant mice were garvage-fed with tamoxifen (75 mg/kg, body weight) twice at an interval of 10 h. In adult mice, tamoxifen was administered intraperitoneally (i.p.) twice a day for 5 days (40 mg/kg, body weight). For BrdU (100 mg/ml in PBS) labeling, adult mice were given (i.p.) the drug twice a day for 2 days (50 mg/kg, body weight); after 3 days, the mice began the 5-day regimen of tamoxifen injections.

Reporter mice and animal care

For LacZ assay, a *Rosa*26-*LacZ* reporter mouse was used. For other assays, a *Rosa26-EYFP* reporter mouse [29] and *Thy1-EYFP* reporter mouse [41] were used. Transgenic mice were raised in a SPF barrier system. At the age of 6 weeks, experiment mice were

transferred to a standard housing space. Both housing spaces are supplied with sterile water and general food, with an auto-switch of day/night (12 h/12 h) control and room temperature control (22 °C). The use of mice, surgery and sacrifice procedures are approved by institutional animal care and use committee (IACUC).

Immunofluorescence

Mice were anesthetized with 20% chloral hydrate, perfused with 40 ml 0.9% NaCl solution and fixed with 25 ml of 4% PFA in PBS (pH 7.4). Mouse brains were fixed in 4% PFA solution for another 24 h, and saturated in 15% to 30% sucrose solution. Coronal brain slices (30 μm) were sectioned using a microtome.

Immunofluorescence was done as previously described [23]. For some experiments, cell nuclei were also labeled by incubating slices in Hoechst solution for 10 min before mounting. The primary antibodies used were: rabbit anti-GFP (1:2 000, Invitrogen), goat anti-DCX (1:200, Santa Cruz Biotechnology), mouse anti-NeuN (1:200, Chemicon), mouse anti-Parvalbumin (1:1 000, Chemicon), mouse anti-GFAP (1:1 000, Chemicon), rabbit anti-Ki67 (1:1 000, Novacastra) and rabbit anti-Tbr2 (1:500, Millipore). YFP was visualized using anti-GFP in all co-labeling experiments, with the exception of those using Ki67 and Tbr2 antibodies, wherein endogenous YFP fluorescence was visualized. The secondary antibodies (1 μg/ml; Molecular Probes) used were: Alexa Fluor 488 donkey anti-rabbit, Alexa Fluor 568 donkey anti-goat and Alexa Fluor 568 donkey anti-mouse.

For BrdU immunostaining, prior to blocking, slices permeated with Triton X-100 were incubated in NCF buffer (0.3 M NaCl, 30 mM citrate buffer (pH 7.0) and 50% formamide) for 2 h at 65 °C, followed by rinsing in NC solution (0.3 M NaCl, 30 mM citrate buffer (pH 7.0)). Slices were then treated with 2 N HCl at 37 °C for 30 min, and neutralized in 0.1 M borate buffer (pH 8.5) for 10 min.

Confocal microscope and neurolucida imaging

Z-stacks of images taken at 0.5-μm intervals through 30 μm coronal slices were acquired and photographed under the 40× oil objective lens of a Zeiss LSM 510 confocal microscope equipped with 488 nm, 543 nm and 633 nm lasers. For cell type identity analysis, brain slices from two mice sacrificed at 14 days post tamoxifen injection (dpi) were used. For each co-labeling experiment, at least six slices per mouse from the anterior, middle and posterior regions of the hippocampus were analyzed. For the differentiation kinetics analysis of YFP^+ cells, at least three mice were analyzed at each time point, using six brain slices per mouse from the anterior, middle and posterior regions of the hippocampus. Cells in the SGZ, GCL and inner hilar region were counted. A few cells with atypical neuronal morphology were observed in the CA3-hilar border; these were excluded from the counting.

For dendrite, spine and bouton imaging, z-stacks of images taken at intervals of 0.4 μm through 30 μm coronal slices were acquired using a 100× oil objective lens. Lower resolution images of dendrites and boutons were acquired at resolution of 0.13 μm × 0.13 μm per pixel. For high-resolution images of single dendrite segments, images were acquired at a resolution of 0.06 μm × 0.06 μm per pixel. For each time point, at least three mice were used; images from three separate slices per mouse and one neuron per slice were collected. For spine quantifications, a secondary or tertiary branch of an apical dendrite was randomly selected. Spines were counted manually using Neurolucida software, and the density was determined by dividing total spine number by length of dendritic segments [18].

Slice preparation and electrophysiology

Brain slices from mice at indicated ages were prepared as previously described [47]. Mice were intra-thoracic perfused with pre-chilled ACSF, mended brain was then sectioned with Leica VT 1000S. Slices were incubated in ACSF (in mM: 119 NaCl, 2.3 KCl, 1.3 $MgSO_4$, 2.5 $CaCl_2$, 26.2 $NaHCO_3$, 1 NaH_2PO_4 and 11 glucose) bubbled continuously with carbogen (95% O_2 plus 5% CO_2). After equilibration for 60 min at 34 °C, slices were transferred to a submerged chamber perfused continuously with arbogenated ACSF at 30 °C via an automatic temperature controller (Warner Instrument Corporation). Control or EYFP-expressing neurons in DG of hippocampus were visualized via green fluorescence and infrared filter. Whole-cell patch clamp recordings were performed under an Axon 700B automatic amplifier (Molecular Devices). Recording pipettes with resistance of 5-7 MΩ were pulled from borosilicate glass (P-97; Sutter Instruments) and filled with intracellular solution of (in mM; 130 potassium gluconate, 10 KCl, 2 $MgCl_2$, 0.2 EGTA, 10 HEPES, 2 ATP and 0.5 GTP). Action potential was measured in current clamp model and depolarization was induced by injection of gradient currents. Membrane resistance and time constant were measured as previously described [35]. Data were analyzed with Clampfit 9.0 and Igor 4.09 (Wavemetrics, Lake Oswego).

Statistics

All data are presented as mean±s.e.m and all statistical analyses were done using one-way ANOVA.

Acknowledgment

We thank Dr Shiaoching Gong (Rockefeller University, USA) for technique advice on BAC recombination, Drs Yang Zhou and Shan He for electrical recording, Mr Yong-chuan Zhu for help on plasmid preparation, Mr Hai-feng Liu for help on mice genotyping, Mr Fu-lin Yang for help on mice management and Dr Qian Hu for the help with confocal imaging. We also thank Miss Ting-Jia Lu for comment on the manuscript. This work was supported by grants from "Chief Scientist Program" of Shanghai Institutes for Biological Sciences, Chinese Academy of Sciences (SIBS2008003), National Basic Research Program of China (2006CB806600), the Key State Research Program of China (2006CB943900) and the Innovative Research Group of the National Natural Science Foundation of China (30721004) to Zhi-Qi Xiong.

References

1 Lie DC, Song H, Colamarino SA, Ming GL, Gage FH. Neurogenesis in the adult brain: new strategies for central nervous system diseases. *Annu Rev Pharmacol Toxicol* 2004; **44**:399-421.

2 Gould E. How widespread is adult neurogenesis in mammals? *Nat Rev Neurosci* 2007; **8**:481-488.

3 Ming GL, Song H. Adult neurogenesis in the mammalian central nervous system. *Annu Rev Neurosci* 2005; **28**:223-250.

4 Lledo PM, Alonso M, Grubb MS. Adult neurogenesis and functional plasticity in neuronal circuits. *Nat Rev Neurosci* 2006; **7**:179-193.
5 Zhao C, Deng W, Gage FH. Mechanisms and functional implications of adult neurogenesis. *Cell* 2008; **132**:645-660.
6 Gheusi G, Cremer H, McLean H, *et al.* Importance of newly generated neurons in the adult olfactory bulb for odor discrimination. *Proc Natl Acad Sci USA* 2000; **97**:1823-1828.
7 Shingo T, Gregg C, Enwere E, *et al.* Pregnancy-stimulated neurogenesis in the adult female forebrain mediated by prolactin. *Science* 2003; **299**:117-120.
8 Santarelli L, Saxe M, Gross C, *et al.* Requirement of hippocampal neurogenesis for the behavioral effects of antidepressants. *Science* 2003; **301**:805-809.
9 Shors TJ, Miesegaes G, Beylin A, *et al.* Neurogenesis in the adult is involved in the formation of trace memories. *Nature* 2001; **410**:372-376.
10 Imayoshi I, Sakamoto M, Ohtsuka T, *et al.* Roles of continuous neurogenesis in the structural and functional integrity of the adult forebrain. *Nat Neurosci* 2008; **11**:1153-1161.
11 Kempermann G, Jessberger S, Steiner B, Kronenberg G. Milestones of neuronal development in the adult hippocampus. *Trends Neurosci* 2004; **27**:447-452.
12 Kempermann G, Gast D, Kronenberg G, Yamaguchi M, Gage FH. Early determination and long-term persistence of adult-generated new neurons in the hippocampus of mice. *Development* 2003; **130**:391-399.
13 Ribak CE, Seress L, Amaral DG. The development, ultrastructure and synaptic connections of the mossy cells of the dentate gyrus. *J Neurocytol* 1985; **14**:835-857.
14 Hetherington PA, Austin KB, Shapiro ML. Ipsilateral associational pathway in the dentate gyrus: an excitatory feedback system that supports N-methyl-D-aspartate-dependent long-term potentiation. *Hippocampus* 1994; **4**:422-438.
15 Jackson MB, Scharfman HE. Positive feedback from hilar mossy cells to granule cells in the dentate gyrus revealed by voltage-sensitive dye and microelectrode recording. *J Neurophysiol* 1996; **76**:601-616.
16 Li G, Berger O, Han SM, *et al.* Hilar mossy cells share developmental influences with dentate granule neurons. *Dev Neurosci* 2008; **30**:255-261.
17 Larimer P, Strowbridge BW. Representing information in cell assemblies: persistent activity mediated by semilunar granule cells. *Nat Neurosci* 2010; **13**:213-222.
18 Zhao C, Teng EM, Summers RG Jr, Ming GL, Gage FH. Distinct morphological stages of dentate granule neuron maturation in the adult mouse hippocampus. *J Neurosci* 2006; **26**:3-11.
19 Overstreet LS, Hentges ST, Bumaschny VF, *et al.* A transgenic marker for newly born granule cells in dentate gyrus. *J Neurosci* 2004; **24**:3251-3259.
20 Feil R, Wagner J, Metzger D, Chambon P. Regulation of Cre recombinase activity by mutated estrogen receptor ligand-binding domains. *Biochem Biophys Res Commun* 1997; **237**:752-757.
21 Lagace DC, Whitman MC, Noonan MA, *et al.* Dynamic contribution of nestin-expressing stem cells to adult neurogenesis. *J Neurosci* 2007; **27**:12623-12629.
22 Lewis PF, Emerman M. Passage through mitosis is required for oncoretroviruses but not for the human immunodeficiency virus. *J Virol* 1994; **68**:510-516.
23 Brown JP, Couillard-Despres S, Cooper-Kuhn CM, *et al.* Transient expression of doublecortin during adult neurogenesis. *J Comp Neurol* 2003; **467**:1-10.
24 Gleeson JG, Lin PT, Flanagan LA, Walsh CA. Doublecortin is a microtubule-associated protein and is expressed widely by migrating neurons. *Neuron* 1999; **23**:257-271.
25 Rao MS, Shetty AK. Efficacy of doublecortin as a marker to analyse the absolute number and dendritic growth of newly generated neurons in the adult dentate gyrus. *Eur J Neurosci* 2004; **19**:234-246.
26 Seki T. Expression patterns of immature neuronal markers PSA-NCAM, CRMP-4 and NeuroD in the hippocampus of young adult and aged rodents. *J Neurosci Res* 2002; **70**:327-334.
27 Heintz N. BAC to the future: the use of BAC transgenic mice for neuroscience research. *Nat Rev Neurosci* 2001; **2**:861-870.
28 Feng G, Mellor RH, Bernstein M, *et al.* Imaging neuronal subsets in transgenic mice expressing multiple spectral variants of GFP. *Neuron* 2000; **28**:41-51.
29 Srinivas S, Watanabe T, Lin CS, *et al.* Cre reporter strains produced by targeted insertion of EYFP and ECFP into the ROSA26 locus. *BMC Dev Biol* 2001; **1**:4.
30 Carleton A, Petreanu LT, Lansford R, Alvarez-Buylla A, Lledo PM. Becoming a new neuron in the adult olfactory bulb. *Nat Neurosci* 2003; **6**:507-518.
31 Pekcec A, Loscher W, Potschka H. Neurogenesis in the adult rat piriform cortex. *Neuroreport* 2006; **17**:571-574.
32 Bernier PJ, Bedard A, Vinet J, Levesque M, Parent A. Newly generated neurons in the amygdala and adjoining cortex of adult primates. *Proc Natl Acad Sci USA* 2002; **99**:11464-11469.
33 Kokoeva MV, Yin H, Flier JS. Neurogenesis in the hypothalamus of adult mice: potential role in energy balance. *Science* 2005; **310**:679-683.
34 Jessberger S, Toni N, Clemenson GD Jr, Ray J, Gage FH. Directed differentiation of hippocampal stem/progenitor cells in the adult brain. *Nat Neurosci* 2008; **11**:888-893.
35 Schmidt-Hieber C, Jonas P, Bischofberger J. Enhanced synaptic plasticity in newly generated granule cells of the adult hippocampus. *Nature* 2004; **429**:184-187.
36 Ge S, Yang CH, Hsu KS, Ming GL, Song H. A critical period for enhanced synaptic plasticity in newly generated neurons of the adult brain. *Neuron* 2007; **54**:559-566.
37 van Praag H, Schinder AF, Christie BR, *et al.* Functional neurogenesis in the adult hippocampus. *Nature* 2002; **415**:1030-1034.
38 Bonfanti L. PSA-NCAM in mammalian structural plasticity and neurogenesis. *Prog Neurobiol* 2006; **80**:129-164.
39 Cameron HA, Woolley CS, McEwen BS, Gould E. Differentiation of newly born neurons and glia in the dentate gyrus of the adult rat. *Neuroscience* 1993; **56**:337-344.
40 Dayer AG, Ford AA, Cleaver KM, Yassaee M, Cameron HA. Short-term and long-term survival of new neurons in the rat dentate gyrus. *J Comp Neurol* 2003; **460**:563-572.
41 Buffelli M, Burgess RW, Feng G, *et al.* Genetic evidence that relative synaptic efficacy biases the outcome of synaptic competition. *Nature* 2003; **424**:430-434.

42 Forster E, Zhao S, Frotscher M. Laminating the hippocampus. *Nat Rev Neurosci* 2006; **7**:259-267.
43 Lynch WP, Brown WJ, Spangrude GJ, Portis JL. Microglial infection by a neurovirulent murine retrovirus results in defective processing of envelope protein and intracellular budding of virus particles. *J Virol* 1994; **68**:3401-3409.
44 Kronenberg G, Reuter K, Steiner B, *et al.* Subpopulations of proliferating cells of the adult hippocampus respond differently to physiologic neurogenic stimuli. *J Comp Neurol* 2003; **467**:455-463.
45 Nimchinsky EA, Sabatini BL, Svoboda K. Structure and function of dendritic spines. *Annu Rev Physiol* 2002; **64**:313-353.
46 Toni N, Laplagne DA, Zhao C, *et al.* Neurons born in the adult dentate gyrus form functional synapses with target cells. *Nat Neurosci* 2008; **11**:901-907.
47 Zhou Y, Wu H, Li S, *et al.* Requirement of TORC1 for late-phase long-term potentiation in the hippocampus. *PLoS ONE* 2006; **1**:e16.

(**Supplementary information** is linked to the online version of the paper on the *Cell Research* website.)